Breast Cancer: Computer-aided Detection with Digital Breast Tomosynthesis[1]

Lia Morra, PhD
Daniela Sacchetto, MSc
Manuela Durando, MD
Silvano Agliozzo, PhD
Luca Alessandro Carbonaro, MD
Silvia Delsanto, PhD
Barbara Pesce, MD
Diego Persano, PhD
Giovanna Mariscotti, MD
Vincenzo Marra, MD
Paolo Fonio, MD
Alberto Bert, PhD

Purpose: To evaluate a commercial tomosynthesis computer-aided detection (CAD) system in an independent, multicenter dataset.

Materials and Methods: Diagnostic and screening tomosynthesis mammographic examinations (n = 175; cranial caudal and mediolateral oblique) were randomly selected from a previous institutional review board–approved trial. All subjects gave informed consent. Examinations were performed in three centers and included 123 patients, with 132 biopsy-proven screening-detected cancers, and 52 examinations with negative results at 1-year follow-up. One hundred eleven lesions were masses and/or microcalcifications (72 masses, 22 microcalcifications, 17 masses with microcalcifications) and 21 were architectural distortions. Lesions were annotated by radiologists who were aware of all available reports. CAD performance was assessed as per-lesion sensitivity and false-positive results per volume in patients with negative results.

Results: Use of the CAD system showed per-lesion sensitivity of 89% (99 of 111; 95% confidence interval: 81%, 94%), with 2.7 ± 1.8 false-positive rate per view, 62 of 72 lesions detected were masses, 20 of 22 were microcalcification clusters, and 17 of 17 were masses with microcalcifications. Overall, 37 of 39 microcalcification clusters (95% sensitivity, 95% confidence interval: 81%, 99%) and 79 of 89 masses (89% sensitivity, 95% confidence interval: 80%, 94%) were detected with the CAD system. On average, 0.5 false-positive rate per view were microcalcification clusters, 2.1 were masses, and 0.1 were masses and microcalcifications.

Conclusion: A digital breast tomosynthesis CAD system can allow detection of a large percentage (89%, 99 of 111) of breast cancers manifesting as masses and microcalcification clusters, with an acceptable false-positive rate (2.7 per breast view). Further studies with larger datasets acquired with equipment from multiple vendors are needed to replicate the findings and to study the interaction of radiologists and CAD systems.

[1] From the Department of Research and Development, im3D, Via Lessolo 3, 10153 Turin, Italy (L.M., D.S., S.A., S.D., D.P., A.B.); Department of Radiology, University of Turin, Turin, Italy (M.D., G.M., P.F.); Department of Diagnostic Imaging and Radiation Therapy, Radiology University of Torino, Azienda Ospedaliero Universitaria Città della Salute e della Scienza di Torino, Turin, Italy (M.D., G.M., P.F.); Unità di Radiologia, IRCCS Policlinico S. Donato, Milan, Italy (L.C.); C.d.C. Paideia, Rome, Italy (B.P.); and Department of Radiology, Sant'Anna Hospital, Turin, Italy (V.M.). From the 2013 RSNA Annual Meeting. Received September 30, 2014; revision requested November 17; revision received December 31; accepted January 22, 2015; final version accepted February 19. **Address correspondence to** L.M. (e-mail: *lia.morra@i-m3d.com*).

Mammography is considered the most cost-effective screening method for early detection of breast cancer. However, the masking effect caused by tissue superposition affects both its sensitivity and specificity. In three-dimensional digital breast tomosynthesis (DBT), multiple projections are acquired at a short angle to reconstruct multiple images at different depths, thus effectively limiting tissue superposition at a relatively low dose of radiation (comparable to that of digital mammography) (1). In retrospective and prospective reader studies (2–4), DBT has shown great potential as a complement to and a possible substitute for digital mammography, yielding both a decreased recall rate and increased sensitivity, especially in women with dense breasts. The popularity of DBT among radiologists is thus increasing; in a recent US survey (5), 30% of interviewed radiologists routinely performed DBT and more than 30% were planning to acquire DBT equipment.

DBT certainly improves visualization of masses and architectural distortions; the margins are more clearly visible, and the masking effect of superimposing glandular tissue is greatly diminished. Early reports showed that DBT might not be as effective for the detection of microcalcification clusters as it is for masses (6); searching for microcalcification clusters could be more difficult for the radiologist because clusters are separated in several different sections, and individual calcifications might be less conspicuous than they are in full-field digital mammography. However, more recent study results (4) have shown no difference between DBT and full-field digital mammography in the rate of detection of in situ cancer.

One of the main concerns about the adoption of DBT technology on a large scale is its potential effect on the workload of radiologists, especially in a screening context. Because a typical DBT view consists of an average of 60 1-mm sections (usually 30–80 sections, depending on breast thickness), interpretation time can be double that with conventional mammography, increasing costs, and possibly, errors due to reader fatigue (7,8).

Computer-aided detection (CAD) systems could be important in the interpretation of DBT images, aiding radiologists to detect lesions more effectively and efficiently. However, to our knowledge, at present, few articles on CAD systems for DBT are available in the literature, and most of them are focused on mass detection, with limited datasets (9–12). The purpose of this study was to evaluate performance (sensitivity and specificity) with a commercial tomosynthesis CAD system in an independent, multicenter dataset.

Advances in Knowledge

- Our study results showed that a digital breast tomosynthesis computer-aided detection system can allow detection of a large percentage (89%, 99 of 111) of breast masses and/or microcalcifications, with an acceptable false-positive rate (2.7 per breast view).
- Overall, computer-aided detection systems allowed detection of 37 of 39 microcalcification clusters (95% sensitivity, 95% confidence interval: 81%, 99%) and 79 of 89 masses (89% sensitivity, 95% confidence interval: 80%, 94%).

Materials and Methods

CAD software, technical support, and statistical consultancy for the study were provided by im3D (Torino, Italy). Three of the authors (L.M., D.S., and S.D.) are researchers at im3D, two authors (D.P. and S.A) are former employees of im3D, and two authors (A.B., a former employee of im3D, and L.C.) are consultants for im3D. Authors V.M. and M.D., who are not consultants or employees in the industry, had control of all included data and data submitted for publication. Mammographic examinations included in this study were randomly selected from a previous institutional review board–approved prospective trial, and all subjects gave informed consent.

Implication for Patient Care

- A digital breast tomosynthesis computer-aided detection system may help radiologists achieve a more accurate and faster interpretation of digital breast tomosynthesis images.

Dataset

The CAD digital tomosythesis system (CAD Breast DTS v2.2, research version; im3D, Torino, Italy) was tested retrospectively in a dataset including 175 patients, of whom 123 patients had histologically proven, screening-detected malignant lesions and 52 had normal results, without benign or malignant lesions and with at least 1 year of negative results at follow-up. All datasets included cranial caudal and mediolateral oblique two-dimensional mammographic and DBT views acquired with a mammographic unit (Selenia Dimensions; Hologic, Bedford, Mass). All examinations were not previously viewed with the CAD system, and a separate dataset was used for training.

The 123 patients with positive results were examined in three different clinical centers. Of these, 106 patients were randomly selected from women who self-referred for mammography

Published online before print
10.1148/radiol.2015141959 **Content codes:** BR DM

Radiology 2015; 000:1–8

Abbreviations:
CAD = computer-aided detection
CI = confidence interval
DBT = digital breast tomosynthesis

Author contributions:
Guarantors of integrity of entire study, D.P., V.M., P.F.; study concepts/study design or data acquisition or data analysis/interpretation, all authors; manuscript drafting or manuscript revision for important intellectual content, all authors; approval of final version of submitted manuscript, all authors; agrees to ensure any questions related to the work are appropriately resolved, all authors; literature research, L.M., S.D., D.P., V.M., P.F., A.B.; clinical studies, M.D., L.A.C., B.P., G.M., V.M., P.F., A.B.; experimental studies, L.M., S.A., V.M., P.F.; statistical analysis, L.M., D.S., S.D., D.P., V.M., P.F.; and manuscript editing, L.M., M.D., S.A., L.A.C., S.D., G.M., V.M., P.F., A.B.

Conflicts of interest are listed at the end of this article.

for subjective symptoms, follow-up after breast surgery, or spontaneous screening at Azienda Ospedaliero Universitaria Città della Salute e della Scienza, Molinette, Turin, and Clinica Paideia, Rome; 17 consecutive patients were recalled for further work-up as part of the regional screening program at Azienda Ospedaliero Universitaria Città della Salute e della Scienza, Sant'Anna, Turin. Subject age ranged from 36 to 87 years (mean ± standard deviation, 60 years ± 13). In the 123 examinations with positive results, 111 malignant masses and microcalcification clusters (72 masses, 22 microcalcification clusters, and 17 masses with microcalcifications) and 21 architectural distortions were detected. Of the 123 examinations with positive results, seven examinations showed two lesions and one examination showed three lesions (one patient with bilateral cancer; one with bifocal cancer; one with ductal carcinoma in situ, which appeared as two separate clusters at DBT; and five with multiple cancers: one patient with three lesions and four patients with two). All cancers were proven at final histologic or microhistologic examination. Examinations showed masses or microcalcification clusters and included 75 invasive ductal carcinomas, 15 ductal carcinomas in situ, 11 invasive lobular carcinomas, and 10 of other types (three mucinous cancers, one apocrine cancer, one mixed lobular and ductal carcinoma, one mixed ductal and micropapillary carcinoma, two nonspecific carcinomas, one tubular carcinoma, and one invasive ductal carcinoma and ductal carcinomas in situ).

Average lesion size ± standard deviation was 23 mm ± 15. Both mediolateral oblique and cranial caudal views were available in most cases (99 lesions) and showed the lesion; in four cases, only the mediolateral oblique projection was available, and eight lesions were visible only on one view. The 52 patients with normal results (44 bilateral and eight unilateral cases, a total of 192 cranial caudal and mediolateral oblique views) were randomly selected from women who self-referred for mammography either for subjective symptoms or spontaneous screening; subjects who underwent previous surgery and/or radiation therapy were excluded. All patients had at least 1 year of follow-up with negative results. Breast density for all patients was assessed by the radiologists who did the retrospective review for the study by using the Breast Imaging Reporting and Data System density categories.

CAD System and Data Analysis

The im3D CAD digital tomosythesis system allows detection of both masses and microcalcification clusters at DBT examination. Projections were first reconstructed by using reconstruction software (Briona 3D; Real Time Tomography, Villanova, Pa); specific reconstruction and postprocessing parameters were selected for both masses and microcalcifications to optimize CAD system performance. Two-dimensional mammographic images were not used at all with the CAD system.

Candidate masses and microcalcification clusters were then separately segmented by using proprietary algorithms, and for each lesion type, a false-positive reduction step was applied and a score was assigned to each candidate. No specific algorithm was included for the detection of architectural distortions, but because the segmentation of masses was reliant on the detection of both opacity and spiculations, CAD system performance on architectural distortions also was registered. CAD operating points for both masses and microcalcification clusters were identified in a separate training dataset of 132 examinations. Microcalcifications superimposed by at least 20% with a mass were merged to yield a single candidate representing a mass with associated calcifications. Finally, the CAD system automatically generated bounding boxes around the segmented candidates, as shown in the Figure. A label was attached to each CAD marker to specify the candidate type (eg, mass or microcalcification clusters), and each candidate was given an identification number.

A radiologist (L.A.C. or E.R., with at least 4 years of experience in digital mammography) annotated lesions by drawing a three-dimensional bounding box in the CAD workstation on the basis of all information available for the case, including mammographic, ultrasonographic (available in all cases), and biopsy reports. The radiologist was instructed to draw the bounding box as close as possible to the lesion, including spiculations; a two-dimensional bounding box was initially drawn on the central section and then extended to all the sections in which the lesion was visible and in focus. For masses with associated calcifications, the same bounding box was used for matching both mass and microcalcification candidates. Matching criteria were as follows: A mass or architectural distortion was detected if the radiologist's bounding box overlapped with a mass CAD bounding box (or a combination of) by at least 6% in volume and 20% along the direction perpendicular to the detector; a microcalcification cluster was detected if at least two calcifications segmented by the CAD system lay within the radiologist's bounding box. Such criteria were empirically determined in a separate dataset to minimize the chance of mismatches. All other CAD candidates were counted as false-positive results. A lesion was considered detected if it was identified with the CAD system in the cranial caudal or mediolateral oblique views or both. In the assessment of sensitivity for masses or microcalcification clusters, only corresponding CAD candidates were considered; in other words, a lesion that appeared as a mass with no associated calcifications was considered detected only if it was marked by the CAD system as a mass, and vice versa. However, masses with associated calcifications were considered detected if the CAD system marked at least a microcalcification cluster or a mass.

Statistical Analysis

Per-lesion sensitivity and associated 95% confidence intervals (CIs) were calculated after the CAD candidates and radiologists' bounding boxes were automatically matched, both including and excluding architectural distortions. Specificity

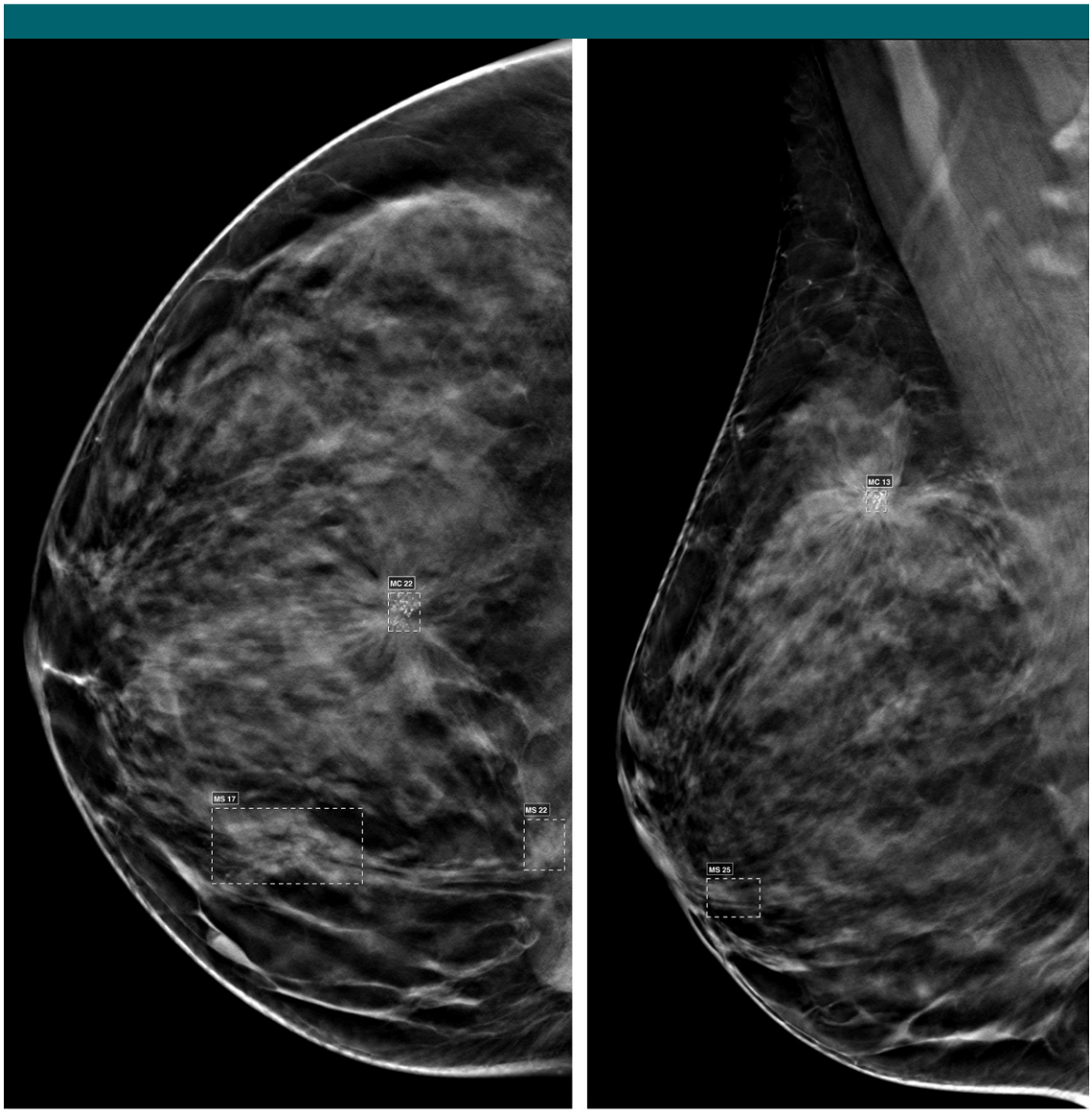

a. **b.**

Digital breast tomosynthesis images in a 38-year-old woman with a 12-mm invasive ductal carcinoma with a spiculated mass with associated calcifications show sections in **(a)** cranial caudal and **(b)** mediolateral oblique orientations, with superimposed CAD markers.
(continues)

was studied by calculating the number of false-positive results per breast view. Other authors (10,11,13) have reported differences between the number of false-positive results observed in patients with positive results compared with those in patients with normal results; therefore, the false-positive rate for patients with negative results also was assessed and reported separately.

Results were stratified by lesion type, histologic result, size, and breast density. The Fisher exact test was used to assess differences in sensitivity between lesion types (masses vs microcalcification clusters), breast density, and indication for mammography (self-referral for symptoms or spontaneous screening vs screening recall). A P value of .05 or lower was considered to indicate a significant difference. Characteristics of lesions missed by the CAD system were visually assessed by a researcher (L.M., with at least 6 years of experience in breast CAD research).

Results

Distribution of breast density in the dataset is available in Table 1. Overall,

(continued)

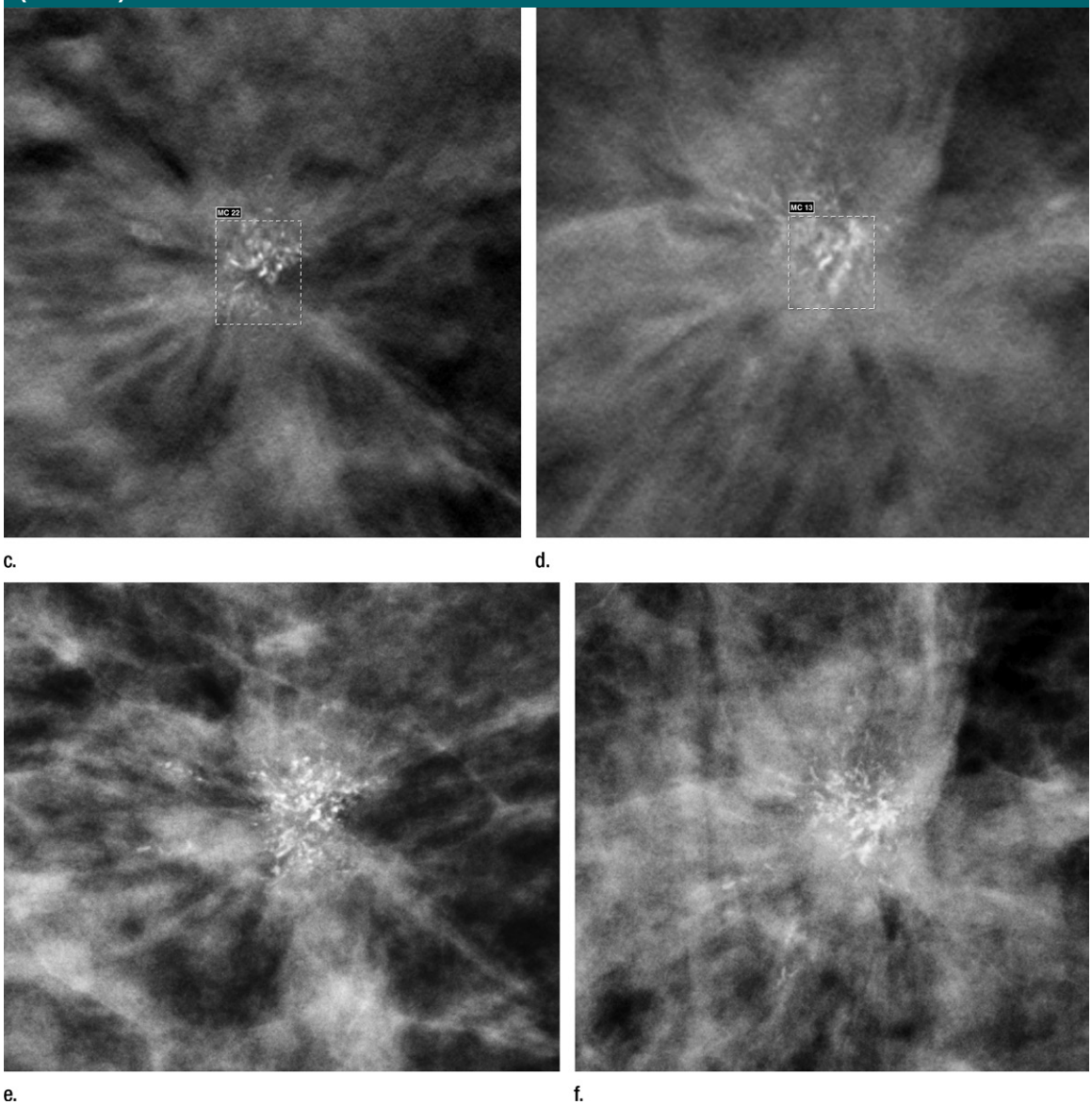

(continued): Close-up images show representative tomosynthesis sections in **(c)** cranial caudal and **(d)** mediolateral oblique orientations. **(e, f)** Two-dimensional mammographic images show corresponding lesion for comparison. Three additional markers were identified by CAD system as false-positive masses.

44% (77 of 135) of the overall dataset, and 35% (seven of 17) of the screening subset were patients with high breast density. For masses and calcification clusters, per-lesion sensitivity with the CAD system was 89% (99 of 111; 95% CI: 82%, 94%); 62 of 72 lesions detected with the CAD system were masses, 20 of 22 lesions detected were microcalcification clusters, and 17 of 17 masses had associated microcalcifications. Of the 99 lesions visible on images from both views, 63 were detected on both views, 17 were detected on the cranial caudal view only, 11 were detected on the mediolateral oblique view only, and eight were not detected with CAD; three of eight lesions detected with the CAD system were visible on one view, and four of four lesions for which only one view was available were detected. Overall, the CAD system showed 37 of 39 (95% sensitivity, 95% CI: 81%, 99%) microcalcification clusters and 79 of 89 (89% sensitivity, 95% CI: 80%, 94%) masses; the differences were not significant (P = .35). All 12 lesions (eight masses and four masses with associated calcifications) in the screening subset were detected with the CAD system;

Table 1

Dataset Composition and Sensitivity Stratified by Breast Density

Parameter	All Breasts	Fatty Breasts	Dense Breasts
No. of patients with malignant lesions	123	63 (34 + 29)*	60 (39 + 21)†
No. of lesions	111	59	52
Masses	72	41	31
Microcalcifications	22	5	17
Masses and microcalcifications	17	13	4
Sensitivity‡	89 (99/111) [82, 94]	93 (55/59) [82, 97]	85 (44/52) [71, 94]
Masses only	86 (62/72) [75, 93]	93 (38/41) [79, 98]	77 (24/31) [58, 89]
Microcalcifications only	91 (20/22) [70, 98]	80 (4/5) [30, 99]	94 (16/17) [70, 99]
Masses and microcalcifications	100 (17/17) [77, 100]	100 (13/13) [72, 100]	100 (4/4) [40, 100]
No. of patients with no lesions	52	14 (4 + 10)*	38 (23 + 15)†
Average no. of false-positive results per breast view§	2.7 ± 1.8 (0–8)	3.1 ± 1.8 (0–7)	2.6 ± 1.8 (0–8)
No. of breast views	192	42	150
With 0 false-positive results	23 (12)	3 (7)	20 (13)
With 1 false-positive results	25 (13)	4 (10)	21 (14)
With 2 false-positive results	44 (23)	9 (21)	35 (23)
With 3 false-positive results	39 (20)	9 (21)	30 (20)
With 4 false-positive results	29 (15)	8 (19)	21 (14)
With 5 false-positive results	15 (8)	5 (12)	10 (7)
With >5 false-positive results	17 (9)	4 (10)	13 (9)

Note.—Unless otherwise indicated, data are number of breast views, with percentage in parentheses.

* Data in parentheses are the number of patients with breast density of D1 and D2, respectively.

† Data in parentheses are the number of patients with breast density of D3 and D4, respectively.

‡ Data are percentages, with numerators and denominators in parentheses and 95% CIs in brackets.

§ Data are averages ± standard deviation, with the range in parentheses.

Table 2

Sensitivity According to Lesion Size and Histopathologic Result

Parameter	No. of Detected Lesions	No. of Lesions	Sensitivity*
Lesion size (cm)			
<1	7	10	70 (40, 90)
1–2	43	50	86 (74, 93)
2–3	28	29	97 (83, 99)
≥3	21	22	95 (77, 99)
Histologic result			
Invasive ductal carcinoma	67	75	89 (80, 95)
Ductal carcinoma in situ	14	15	93 (66, 99)
Invasive lobular carcinoma	9	11	82 (50, 97)
Other	9	10	90 (54, 99)

* Data are percentages, with 95% CIs in parentheses.

sensitivity for screening recalls was not significantly different than sensitivity for women who self-referred for mammography (87 of 99, 88%, $P = .36$). Only two microcalcification clusters were discarded by the CAD system, probably because of the lack of conspicuity compared with the background. Of the 10 masses discarded by the CAD system, one was a satellite lesion of a larger cancer (> 4 cm), four were very close to the image border or the pectoral muscle and visible on one view only, and two were discarded by the CAD system because of oversegmentation.

When architectural distortions were included, the CAD system showed per-lesion sensitivity of 85% (95% CI: 78%, 91%) and 13 of 21 architectural distortions were detected. Results stratified by breast density, lesion type, mammographic lesion size, and histopathologic examination are summarized in Table 1 and Table 2. The observed CAD system sensitivity for masses was 93% (38 of 41) in fatty breasts (D1 and D2) and 77% (24 of 31) in dense breasts (D3 and D4, $P = .09$). Sensitivity for microcalcification clusters was 80% (four of five) and 94% (16 of 17) for fatty and dense breasts, respectively ($P = .35$). Overall, the difference in sensitivity for fatty and dense breasts was not significant ($P = .22$). Sensitivity for small lesions (< 2 cm) was lower than that for larger lesions ($P < .05$).

For the entire dataset, the CAD system yielded an average of 2.6 ± 1.9 (median, 2) false-positive lesions per volume; 0.5 false-positive lesions were microcalcification clusters, 1.9 were masses, and 0.2 were masses with associated microcalcifications. In patients with negative results, the CAD system yielded an average of 2.7 ± 1.8 false-positive lesions; 0.5 false-positive lesions were microcalcification clusters, 2.1 were masses, and 0.1 were masses with associated calcifications (Table 2).

Discussion

Previous research in the field of mammographic CAD was aimed mostly at increasing radiologists' sensitivity and the detection of cancer at an earlier stage of development; therefore, developers aimed for high sensitivity coupled with a low number of false-positive results to minimize their detrimental effects on reader specificity. We envision that the role of CAD systems in DBT probably will be different; compared with full-field digital mammography, DBT yields superior diagnostic performance (both specificity and sensitivity) but poses additional

challenges (mostly an increase in reading time), especially in organized screening programs. From a CAD point of view, DBT may pose a few advantages such as mass margins that are more clearly visible; however, because of the three-dimensional nature of DBT and the presence of artifacts in the direction perpendicular to the detector due to the limited acquisition angle (12), segmentation of both masses and calcifications poses many additional challenges compared with conventional mammography. Moreover, in processing three-dimensional volumes, a high number of false-positive results usually is generated; and hence, it is more difficult to achieve low false-positive rates than it is with two-dimensional imaging.

In the assessment of full-field digital mammographic images, commercial CAD systems usually achieve high sensitivity (94%–96%) for screening-detected lesions, with approximately 2–2.5 false-positive results per examination, corresponding to approximately 0.5 false-positive rate per breast view (13,14). Early reports on CAD systems for DBT reported sensitivity of approximately 90% with one to two false-positive results per breast view for masses (9,12), and 85%–95% sensitivity with 0.7–1.2 false-positive results per breast view for microcalcification clusters (10,11), corresponding to an overall false-positive rate of 2–3 per breast view. Our results were comparable to those with other DBT CAD systems, but were obtained by using a larger, multicenter dataset; furthermore, many of the aforementioned works were preliminary assessments of the technology and did not include performance evaluation on independent testing sets. Consistent with results of previous reports on both full-field digital mammography and DBT CAD, sensitivity was slightly higher for microcalcification clusters than for masses, although the differences were not significant.

Sensitivity for masses appeared to be negatively affected by lesion size and breast density: eight of 12 false-negative lesions were masses smaller than 2 cm. Contrary to results of a previous study (15), we did not observe an effect of lesion histopathologic results, as previously found for mammographic CAD. However, our sample size was too small to observe statistically significant differences and to extract definitive conclusions.

Not surprisingly, density appeared to affect more substantially the identification of masses than that of microcalcifications, but this trend should be verified in a larger sample. We observed a high percentage of dense breasts, which is consistent with our dataset comprising mostly diagnostic examinations; in the screening subset, the proportion of dense breasts was slightly lower than that in the overall dataset. Previous reports (15–18) on mammographic CAD showed similar trends: With increased breast density, sensitivity for microcalcifications does not change, while sensitivity for masses decreases. Differences in overall sensitivity also may depend on changes in the relative prevalence of the different lesion types in dense versus fatty breasts: In the dense breast subset, there was a higher percentage of cancers that appeared as microcalcification clusters (33% vs 9%) and a lower percentage of lesions that appeared as either masses (60% vs 71%) or masses with microcalcifications (8% vs 21%). Finally, in our study, breast density was evaluated by one radiologist, and this limits the validity of our findings because visual assessment shows high interrater variability (19,20). For this reason, comparison of CAD results with automatic breast density calculation would be of particular interest.

As observed with the use of both mammography and DBT CAD systems, the false-positive rate for microcalcification clusters was considerably lower than that for masses. There were small differences in the number of false-positive results between the assessment of patients with lesions and those without lesions, who constitute the majority of real patient populations, especially in a screening scenario. Also, the number of false-positive results was higher for fatty breasts than for dense breasts, although differences were very small.

In the present study, the CAD system, which was not specifically designed for detection of architectural distortion (but takes into account the presence of spiculations in mass detection and characterization), allowed detection of most architectural distortions, but sensitivity remained low compared with that for solid masses. Architectural distortions are a common weak spot also for conventional mammographic CAD systems (21).

This study had limitations. Most of our examinations came from a diagnostic population, thus further studies are needed to assess performance in a screening population. Performance in benign lesions should likewise be assessed. In our dataset, four projections were available only in 63% of the cases, and therefore, it was impossible to assess case-based false-positive rates. As is common in retrospective stand-alone CAD evaluation, sensitivity was assessed in screening-detected cancers; however, increasing radiologists' sensitivity ultimately depends on the CAD system's ability to allow detection of interval cancers. Results of a study (19) in the literature suggest that CAD may have lower sensitivity in interval cancers compared with screening-detected ones. Furthermore, CAD associated with DBT could be important in the reduction of interpretation times. Another limitation of this study is that it included only images from one vendor's equipment.

In conclusion, we showed that a DBT CAD system can allow detection of a large percentage (89%, 99 of 111) of breast masses and/or microcalcifications with an acceptable false-positive rate (2.7 marks per breast view). CAD sensitivity was assessed in a relatively large number of women with biopsy-proven lesions by taking into account clinically relevant factors that included breast density, mammographic presentation, histopathologic results, and lesion size to gain an understanding of how CAD could serve the radiologist in clinical practice. Further prospective reader studies in larger screening populations are needed to study the interaction between CAD and radiologists, and to gain insight on how CAD can contribute to early diagnosis of cancer.

Acknowledgments: We thank all the staff that contributed to data collection for both this study and CAD development, in particular E. Regini,

MD (Department of Diagnostic Imaging and Radiotherapy, Radiology University of Torino, Azienda Ospedaliero-Universitaria Città della Salute e della Scienza di Torino), for help in case annotations. We fondly remember Stefano Ciatto, MD, and the many fruitful discussions about CAD evaluation and its potential role in breast imaging and screening.

Disclosures of Conflicts of Interest: L.M. Activities related to the present article: received personal fees as a researcher for im3D. Activities not related to the present article: disclosed no relevant relationships. Other relationships: disclosed no relevant relationships. **D.S.** Activities related to the present article: received personal fees as a researcher for im3D. Activities not related to the present article: disclosed no relevant relationships. Other relationships: disclosed no relevant relationships. **M.D.** disclosed no relevant relationships. **S.A.** Activities related to the present article: former employee at im3D. Activities not related to the present article: disclosed no relevant relationships. Other relationships: disclosed no relevant relationships. **L.C.** Activities related to the present article: consultancy for im3D. Activities not related to the present article: consultancy for im3D. Other relationships: disclosed no relevant relationships. **S.D.** Activities related to the present article: received personal fees as a researcher for im3D. Activities not related to the present article: received personal fees as a researcher for im3D. Other relationships: disclosed no relevant relationships. **B.P.** disclosed no relevant relationships. **D.P.** Activities related to the present article: disclosed no relevant relationships. Activities not related to the present article: disclosed no relevant relationships. Other relationships: former employee for im3D. **G.M.** disclosed no relevant relationships. **V.M.** disclosed no relevant relationships. **P.F.** disclosed no relevant relationships. **A.B.** Activities related to the present article: received personal fees from im3D. Activities not related to the present article: disclosed no relevant relationships. Other relationships: disclosed no relevant relationships.

References

1. Wu T, Stewart A, Stanton M, et al. Tomographic mammography using a limited number of low-dose cone-beam projection images. Med Phys 2003;30(3):365–380.
2. Ciatto S, Houssami N, Bernardi D, et al. Integration of 3D digital mammography with tomosynthesis for population breast-cancer screening (STORM): a prospective comparison study. Lancet Oncol 2013;14(7):583–589.
3. Skaane P, Bandos AI, Gullien R, et al. Comparison of digital mammography alone and digital mammography plus tomosynthesis in a population-based screening program. Radiology 2013;267(1):47–56.
4. Friedewald SM, Rafferty EA, Rose SL, et al. Breast cancer screening using tomosynthesis in combination with digital mammography. JAMA 2014;311(24):2499–2507.
5. Hardesty LA, Kreidler SM, Glueck DH. Digital breast tomosynthesis utilization in the United States: a survey of physician members of the Society of Breast Imaging. J Am Coll Radiol 2014;11(6):594–599.
6. Spangler ML, Zuley ML, Sumkin JH, et al. Detection and classification of calcifications on digital breast tomosynthesis and 2D digital mammography: a comparison. AJR Am J Roentgenol 2011;196(2):320–324.
7. Dang PA, Freer PE, Humphrey KL, Halpern EF, Rafferty EA. Addition of tomosynthesis to conventional digital mammography: effect on image interpretation time of screening examinations. Radiology 2014;270(1):49–56.
8. Bernardi D, Ciatto S, Pellegrini M, et al. Application of breast tomosynthesis in screening: incremental effect on mammography acquisition and reading time. Br J Radiol 2012; 85(1020):e1174–e1178.
9. Chan HP, Wei J, Zhang Y, et al. Computer-aided detection of masses in digital tomosynthesis mammography: comparison of three approaches. Med Phys 2008;35(9):4087–4095.
10. Sahiner B, Chan HP, Hadjiiski LM, et al. Computer-aided detection of clustered microcalcifications in digital breast tomosynthesis: a 3D approach. Med Phys 2012;39(1):28–39.
11. Samala RK, Chan HP, Lu Y, et al. Computer-aided detection of clustered microcalcifications in multiscale bilateral filtering regularized reconstructed digital breast tomosynthesis volume. Med Phys 2014;41(2):021901.
12. van Schie G, Wallis MG, Leifland K, Danielsson M, Karssemeijer N. Mass detection in reconstructed digital breast tomosynthesis volumes with a computer-aided detection system trained on 2D mammograms. Med Phys 2013;40(4):041902.
13. Yang SK, Moon WK, Cho N, et al. Screening mammography-detected cancers: sensitivity of a computer-aided detection system applied to full-field digital mammograms. Radiology 2007;244(1):104–111.
14. The JS, Schilling KJ, Hoffmeister JW, Friedmann E, McGinnis R, Holcomb RG. Detection of breast cancer with full-field digital mammography and computer-aided detection. AJR Am J Roentgenol 2009;192(2):337–340.
15. Brem RF, Hoffmeister JW, Rapelyea JA, et al. Impact of breast density on computer-aided detection for breast cancer. AJR Am J Roentgenol 2005;184(2):439–444.
16. Malich A, Fischer DR, Facius M, et al. Effect of breast density on computer aided detection. J Digit Imaging 2005;18(3):227–233.
17. Obenauer S, Sohns C, Werner C, Grabbe E. Impact of breast density on computer-aided detection in full-field digital mammography. J Digit Imaging 2006;19(3):258–263.
18. Baker JA, Rosen EL, Lo JY, Gimenez EI, Walsh R, Soo MS. Computer-aided detection (CAD) in screening mammography: sensitivity of commercial CAD systems for detecting architectural distortion. AJR Am J Roentgenol 2003;181(4):1083–1088.
19. Redondo A, Comas M, Macià F, et al. Inter- and intraradiologist variability in the BI-RADS assessment and breast density categories for screening mammograms. Br J Radiol 2012;85(1019):1465–1470.
20. Bernardi D, Pellegrini M, Di Michele S, et al. Interobserver agreement in breast radiological density attribution according to BI-RADS quantitative classification. Radiol Med (Torino) 2012;117(4):519–528.
21. Ciatto S, Ambrogetti D, Bonardi R, et al. Comparison of two commercial systems for computer-assisted detection (CAD) as an aid to interpreting screening mammograms. Radiol Med (Torino) 2004;107(5-6):480–488.